

DMD2011-5230

DESIGN AND TESTING OF A PRESSURE SENSING LAPAROSCOPIC GRASPER

Khashayar Vakili
Department of Surgery
Children's Hospital Boston
Boston, MA 02115

Mattias S Flander
Toomas R Sepp
Manuel Corral
Juan D Diaz
Alexander Slocum
Mechanical Engineering
Department
Massachusetts Institute of
Technology
Cambridge, MA 02139

Grace SL Teo
Brigham and Women's Hospital
Boston, MA 02115

ABSTRACT

In order to improve dexterity and tactile feedback during grasping in laparoscopic surgery, a pressure-sensing, ergonomic laparoscopic grasper with parallel motion grasper jaws has been designed, prototyped, and tested to provide surgeons with a safer and more user-friendly instrument than what is currently available. Parallel motion grasping creates a uniform pressure distribution along the length of the grasper jaws. Moreover, a pressure sensor located in one of the grasper jaws helps surgeons control the pressure applied during grasping. Ease-of-use of the grasper was enhanced through ergonomic handle design. Results from force and motion testing of a 2x prototype of the design were consistent with analytical predictions. These improvements demonstrate that this new laparoscopic grasper can both improve the dexterity of grasping tasks and reduce the incidence of tissue injury during laparoscopic surgery.

INTRODUCTION

A dexterous, pressure-sensing laparoscopic grasper has the potential to enhance laparoscopic surgery by providing the manipulation capabilities associated with open surgery to minimally invasive laparoscopic procedures. While graspers are ideally natural extensions of the surgeon's hand in manipulating tissue, currently available tools significantly diminish the tactile feedback the surgeon receives. Hence, enhanced tactile feedback and grasping ability are important. Tissue trauma due to excessive grasp force is a frequent occurrence, and was the initial motivation for starting this project. Excessive force can damage tissue due to tissue ischemia when blood flow is cut off, or due to mechanical injury. Current graspers also have an unequal pressure distribution across their grasper surfaces since the grasper jaws possess only angular motion similar to that of crocodile jaws.

Tissue grasped in the region of the jaws closer to the shaft inevitably experiences a higher pressure than tissue grasped at the tip of the jaws.

On the other hand, the primary purpose of a laparoscopic grasper is its ability to grasp tissue. Currently available graspers have a tendency to push tissue out of the grasper jaws as they close, due to their non-parallel closing motion. This makes grasping tissue difficult. As a result, tissue can get damaged from repeated attempts to grasp it.

Finally, surgeons which use current graspers for extended periods of time are often subject to hand strain injuries due to handle design. We therefore decided to design a laparoscopic grasper with force feedback in the handle and a more dexterous grasping mechanism. This grasper is accurate and easier to use than a conventional grasper, and the handle is designed with human factors in mind.

DESIGN AND DISCUSSION

Functional Requirements

In light of the existing role of the grasper in surgery and the problems associated with current graspers, a set of functional requirements for a new laparoscopic grasper was determined as follows:

- 1) Grab and move tissue: The grasper should be able to exert sufficient force on tissue to grip and move it with minimal risk of tissue slippage
- 2) Minimal tissue damage: The grasper should possess minimal risk of applying excessive pressure on tissue during grasping
- 3) Small: The grasper should be able to fit through a 5mm trocar
- 4) Safe: The grasper should not pose an increased risk to the patient or surgeon, e.g. risk of electrical burns
- 5) Cost appropriate

Strategies

Two strategies were chosen to fulfill these functional requirements. Firstly, a pressure feedback feature might allow surgeons to better sense and thus control the amount of pressure they apply during grasping. Secondly, we noted that a significant disadvantage of current graspers was the angled grasper jaws that resulted in very uneven pressure distribution across the jaws. An improved design with parallel motion of the grasper jaws would enable the same overall force to be applied to tissue, but with a lower peak pressure at any point.

Pressure feedback has been shown to be important in enhancing grasp control and safety [1-5]. In a study by Delft Institute of Technology of 386 European laparoscopic surgeons, 79% felt necessary to have “new laparoscopic grasper with augmented feedback” while 77% would like to have “tactile feedback as indication of level of pinch force”[6]. When augmented force feedback was provided, a third of subjects, consisting of both experienced and novice surgeons, became dependent on it for laparoscopic grasping [1].

For this reason, several attempts have been made to incorporate force feedback into laparoscopic graspers. Vibrotactile grips, where the handle vibrates upon certain pressures being attained at the grasper jaws have been employed and shown to be useful in aiding safe grasping and education of novice surgeons [1]. Another form of tactile feedback involved using graspers with an extended lever mechanism possessing a high mechanical efficiency of up to 90% [7]. This allowed subjects to ‘feel’ the stiffness of the object being grasped. Unfortunately, subjects found it difficult to exert constant force on tissue, and the actual mechanism is too large and impractical for an actual laparoscopic instrument. Finally, a grasper was also designed with master and slave components at the handle and jaw, respectively, possessing separate motors and controllers. By manipulating finger loops at the handle, the position of the jaws could be controlled. Simultaneously, forces experienced at the jaws are reflected back to the loops [2]. This mechanism required a relatively high amount of circuitry and electronics.

Other attempts at re-design of laparoscopic grasper have focused on reducing the peak pressures experienced unevenly across tissue being grasped. A couple of mechanisms consisting of parallel jaws have been designed and patented [8, 9]. In one embodiment, a 3-fingered parallel mechanism for specialized grasping of large organs similar to the linkage proposed in this paper [9] was described. Another grasper was designed in which grasper jaws were replaced with jointed, finger-like jaws. These jaws reflected the movement of fingers at the handle (which had finger-loops). This allowed bowel to be grasped and suspended from curved ‘fingers’, as in open surgery [10]. Vacuum suction has also been successfully experimented with for reducing tissue trauma, in which the grasper jaws are replaced by a suction device [11]. Finally, peak pressures at the grasper jaws have been shown to be somewhat eliminated by the use of compliant tip made of silicon [12].

Based on the success of previous similar strategies in reducing tissue damage, our final strategy was determined as a pressure feedback system to allow better control over the pressure being exerted and parallel jaw motion for a uniform pressure profile across the grasper jaws. We developed novel concepts to implement these strategies.

Concepts

The rationale for the concepts chosen to implement the strategies is described below. A 2x prototype (scaled up twice from the ideal design, Fig. 1) was built to prove the feasibility of the concepts.

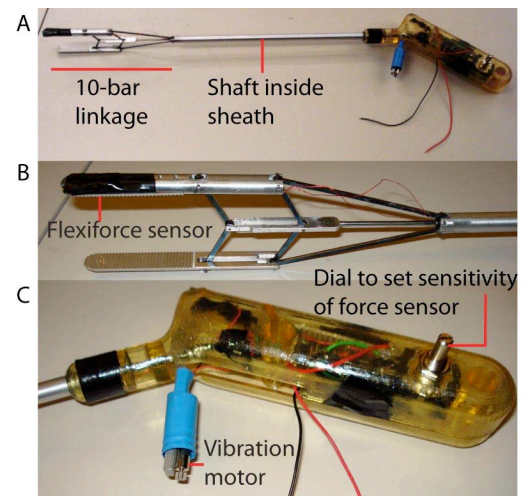


Fig. 1 A 2x prototype of the described grasper was built. The entire grasper (A), close-up of the 10-bar linkage which includes the grasper jaws (B), and handle (C) are shown.

Force feedback Several options were considered for force feedback: Tactile, auditory and visual feedback. Tactile feedback was considered the superior concept of the three as it is the most natural sense for communicating feedback regarding pressure. Although auditory feedback is superior to visual feedback for higher priority signals, ambient noise levels in hospital operating rooms can peak at 65-70dB [13], hence auditory feedback was not used.

Tactile feedback was embodied in our design as vibration. We considered using constant vibration during grasping, which would increase in amplitude as grasping force increased. However, this concept was rejected for several reasons. Firstly, it might be distracting to the surgeon to hold a constantly vibrating instrument. Secondly, detecting slight increases in the amplitude of vibration is difficult. Finally, the current drawn by a combined LED light and vibration motor is an order of magnitude higher than that drawn by the force sensing circuit, making battery drain a potential problem.

After taking these factors into consideration, a vibrating trigger and LED light which would vibrate and light up simultaneously when a pressure threshold was reached was chosen. This allows the grasping force to be monitored by others in the operating room in addition to the user. For our 2x

prototype, a DC vibration motor similar to those found in cell phones was taped to the trigger (Fig. 1c). Trigger vibration was chosen over handle vibration, as the fingers have a higher sensitivity to vibration than the palm, and also to reduce any transmission of vibration to the shaft and grasper jaws. The vibration motor was coupled to a red LED light for visual feedback. The LED light was located at the top of the handle for easy detection.

The sensor used for our prototype was a Flexiforce® Sensor from Tekscan Inc. This is a paper-thin piezoresistive force sensor, which comes in various force ranges and configurations. We used a standard A201-1 model, which has a force range of 0-1 lb (4.4N) [14]. The sensor was mounted in one of the grasper jaws, placing the active sensing area near the tip (Fig. 1b). Since the area of the grasper surface exceeds the active sensing area of the sensor, a small cylindrical shim was fashioned from layered paper and glued to the sensing surface. Ideally, the shim should be attached to the grasper jaw, since uneven glue distribution could create local pressure peaks on the sensor and result in unpredictable force measurements.

Circuit design The circuit was designed to activate the vibration motor and LED light when a certain threshold pressure was exerted by the grasper. For our initial prototype, we used capillary pressure (30 mm-Hg) as a guideline for acceptable grasping pressure. Beyond this pressure, blood supply would theoretically be cut off, leading to tissue ischemia after prolonged periods. Based on this guideline, we developed a circuit that would use a sensor to detect forces normal to the grasper surface on the order of 1 N, allowing us to apply enough pressure to pick up light objects and suspend them without triggering a warning light and vibration. Several parameters can be calibrated to give our desired voltage-force relationship. Mechanically, the pre-loading force on the sensing area and the stiffness of the surface plate can be calibrated.

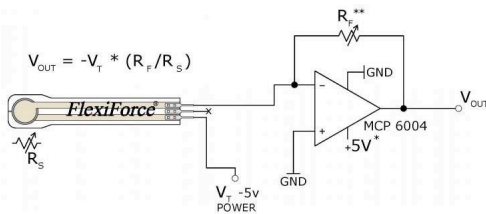


Fig. 2 Flexiforce® recommended drive circuit [14]

Fig. 2 shows Tekscan’s recommended driving circuit for this sensor[14]. The sensitivity of the force measurement can be increased by increasing the resistance R_F (recommended range is 1- 100kΩ) or by increasing the supply voltage V_T . We operated on a supply voltage of -4.5 V with respect to ground, and $R_T=100k\Omega$. Although we used a constant voltage power supply for testing our circuit, the supply voltage used was +9V to simulate a single 9V battery. A 9V voltage supply was demonstrated as sufficient for this application, and disposable 9V batteries are commercially available. The 9V voltage was

divided, with ground placed at 4.5 V in order to provide both a positive and a negative supply voltage.

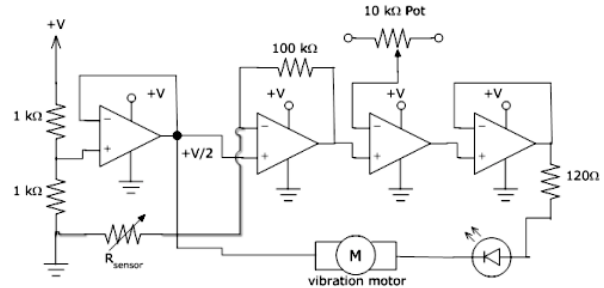


Fig. 3 Full circuit diagram of the designed grasper

To provide feedback above a set pressure threshold, we used an analog comparator, which compares the voltage output of the sensor circuit in Fig. 2 to a reference voltage (Fig. 3). If the sensor circuit outputs a voltage greater than this reference, then the comparator increases its output from +4.5 V to +9V (recall that our ground is placed at +4.5V by virtue of a voltage divider). The DC motor and LED are connected in series between the output of the comparator and ground. As the output of the comparator switches from +4.5 V to +9V, the motor and LED power up, operating on a potential difference of 4.5V until the output of the comparator switches back to a +4.5V output.

The reference voltage of the comparator is regulated by a 10kΩ potentiometer, which is accessible from the outside of the handle, allowing the user to fine-tune the threshold voltage (and consequently the threshold of the grasping force) that powers up the motor and LED. The first and fourth operational amplifiers (from left to right) in Figure 2 are power op amps of the model LM675, serving to buffer the part of the circuit under load from the part of the circuit performing logic operations. Power op amps were used because most precision or general purpose op amps fall short of the required output current of 40-50mA that drives the motor. A small resistor was nonetheless placed in series with the load to limit the current going through to a reasonable value. The second op amp was part of the inverting amplifier circuit recommended by Tekscan to drive the Flexiforce sensor. A high precision op amp (LT1001) was used for this circuit to ensure fast response times and eliminate the need to trim offsets. Finally, the third “op amp” in the diagram is an integrated comparator chip (LM111), whose function has already been covered. The DC motor is similar to that used for cell-phone vibrators.

Handle ergonomics Although our main aim in designing a new laparoscopic grasper was to avoid unnecessary trauma to the patient, minimizing repetitive stress injuries for surgeons using these graspers was also deemed important. To reduce the risk of such injuries, handles should be ergonomically designed to minimize the need for the hand to deviate from its neutral position [15]. Deviation of the hand from its neutral position is best avoided by angling the handle appropriately [15]. We therefore designed a 45 degree bend in our handle with respect

to the shaft. This allows the user's hand to remain in an approximately neutral position when operating within what we considered the most likely workspace, i.e standing over the patient and moving the handle through small radial and ulnar deviations of the hand to access all regions of the patient's abdomen.

In addition to the strain injuries that the current "scissor grip" design may cause, we also found that such current grasper handles (Fig. 4A) are inherently ill-balanced. During grasping, the entire hand moves, causing the end effector of the instrument to rise and fall in synchrony, unless supported by a trocar or some other rigid support. In contrast, our design allows the handle to be propped against the palm of the hand, while one or two fingers actuate the grasping motion by pulling on a trigger (Fig. 4B). The end effector of the grasper remains immobile, allowing the user to actuate the grasper without undesired motion of the grasper shaft.

A: Current 'Scissor-grip' grasper handle



B: Proposed ergonomic grasper handle

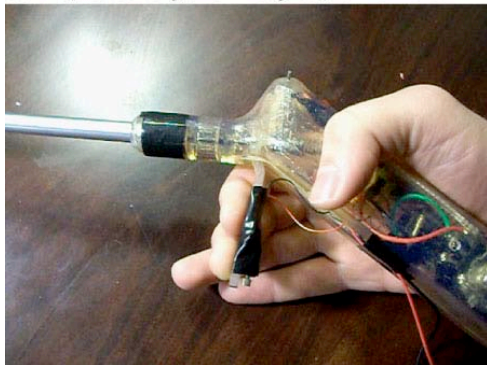


Fig. 4 Handle design. A typical current 'scissor-grip' grasper handles is shown (A) [16], for comparison to our ergonomically designed grasper handle (B).

Equal force distribution A 10-bar linkage was designed to implement parallel motion of grasper jaws with respect to each other (Fig. 5). All joints are pin joints, except for the sliding joint between the sheath and shaft. When the shaft is pushed horizontally forward out of the sheath, the jaws open vertically (Fig. 5A and 5B).

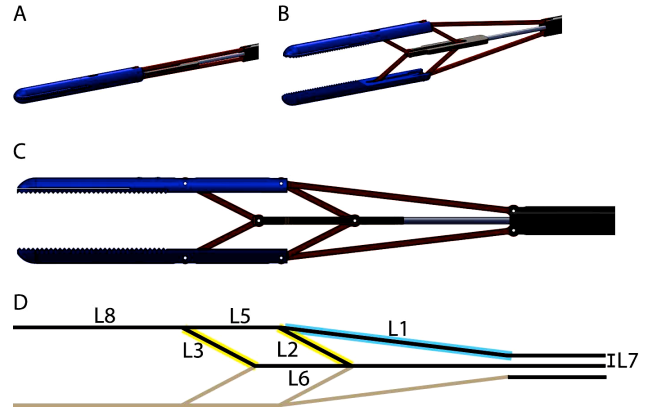


Fig. 5 Illustration of 6-bar linkage mechanism for parallel motion of grasper jaws. SolidWorks assemblies for the linkage in closed (A) and open (B) conformations, and a side profile (C) are shown. A schematic of the linkage (D) is also shown with annotations of different links and/or lengths used in analysis. Note that the 10-bar linkage can be split symmetrically to give a 6-bar linkage (shown in black) on each side, with 2 shared linkages – the shaft and sheath. L2 and L3 (yellow) maintain parallelism of the grasper jaws, while L1 (blue) converts the horizontal motion of the shaft to vertical motion of the grasper jaws by constraining the distance between the grasper jaws and sheath.

The linkage concept for the grasper could be simplified as a 6-bar linkage due to symmetry about the shaft. The linkage has 7 nodes – 6 nodes are pivoting (linkages attached by pin joints), while 1 node is sliding (the shaft slides within the sheath). According to Gruebler's equation for the degrees of freedom, the mechanism has only 1 degree of freedom.

In the 6-bar linkage, 2 of the linkages (L2 and L3) maintain parallelism of the grasper jaws, while one link (L1) constrains the forward motion of the grasper jaws when the shaft moves forward (Fig. 5D)

Analysis of grasper forces and motion

To analyze certain aspects of grasper jaw motion, it was useful to further simplify the linkage into independent groups of linkages. As shown in Fig. 6, analysis of only 4 of the 6 linkages is necessary to obtain a prediction for the (i) height of jaw opening and (ii) backward motion of the jaws as the jaw opens. Similarly, analysis of a different set of 4 linkages is necessary to predict the degree to which the grasper jaws deviate from parallel due to manufacturing errors and movement of linkage heads around pin joints.

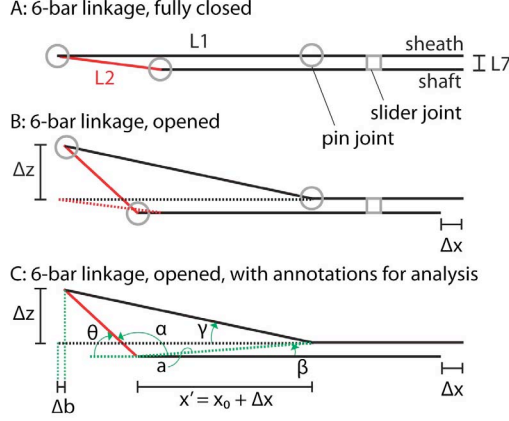


Fig. 6 Illustration of analytical method to find relation between horizontal shaft motion, Δx , jaw opening width, Δz , and backward horizontal motion of grasper jaws during opening, Δb .

Analysis of the height of jaw opening The height of jaw opening, Δz , with respect to the horizontal motion of the shaft, Δx , was solved as shown below and in Fig. 6:

$$a = \sqrt{x'^2 + L7^2} \quad (1)$$

$$\alpha = \cos^{-1} \left[\frac{-L1^2 + a^2 + L2^2}{2 \cdot a \cdot L2} \right] \quad (2)$$

$$\beta = \tan^{-1} \frac{L7}{L1} \quad (3)$$

$$\theta = \pi - \alpha - \beta \quad (4)$$

$$\Delta z = L2 \sin \theta - L7 \quad (5)$$

A plot of Δz against Δx for the 2x prototype is shown in Fig. 7.

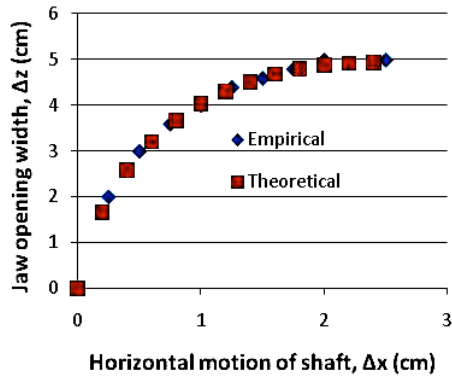


Fig. 7 Plot of the jaw opening width versus forward horizontal motion of the shaft for the 2x prototype. Theoretical predictions and results from empirical testing of the prototype are both shown.

Analysis of the horizontal motion of grasper jaws The link, $L1$, constrains the forward motion of the grasper jaws, such that the forward motion of the shaft is prevented from being transferred to the grasper jaws when the jaws are opened. As a result, the grasper jaws move in a segment of a circular path, for which $L1$ is the radius. When the jaws are opened, the jaws move backwards towards the user (Fig. 6C).

A plot of the backward motion, Δb , against Δz_{\max} , the maximum jaw opening width, is shown in Fig 8, from the equation and in Fig. 6C:

$$\Delta b = L1[1 - \cos \gamma] = L1 \left[1 - \cos \left(\sin^{-1} \frac{\Delta z_{\max}}{L1} \right) \right] \quad (6)$$

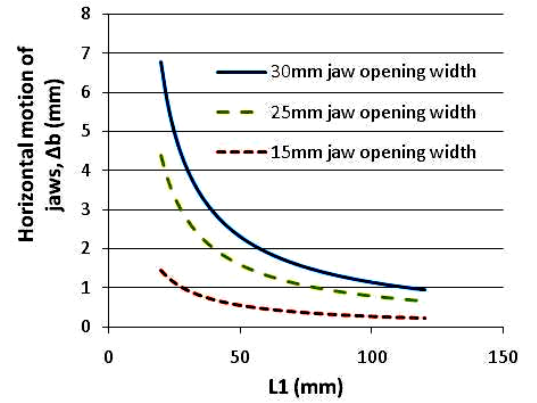


Fig. 8 Plot of the backward horizontal motion of grasper jaws during opening against the length of the link, $L1$, for 3 different maximum jaw opening widths.

As shown in Fig. 8, the horizontal motion of the grasper jaws decreases with both decreasing jaw opening width and $L1$. To limit Δb , $L1$ was chosen to be 39.62mm for a desirable maximum jaw opening height of 25mm, which is similar to the jaw opening width of current graspers.

Analysis of linkage stresses and shaft forces To analyze the stresses experienced by the linkages during grasping, we assumed an overall pressure on the grasper jaw of 30mmHg, which is equal to capillary pressure, the typical threshold for grasping tissue without causing ischemia. From the grasper jaw area, the overall force was calculated to be 0.508N. Linkage stresses were then solved by assuming a force at the tip of the grasper jaw of 0.508N (Fig. 9).

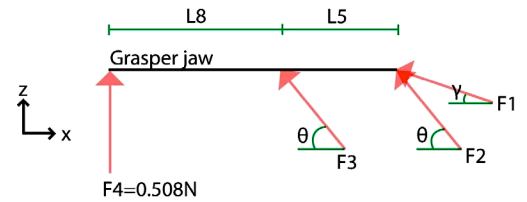


Fig. 9 Schematic of forces acting on grasper jaw.

By summing the moments about the point at which $F1$ and $F2$ acts on the grasper jaw, $F3$ was solved as

$$F3 = -\frac{F4(L8 + L5)}{L5 \sin \theta} \quad (7)$$

By summing the force components in the x-direction, an expression of F1 was obtained as

$$F1 = -(F2 + F3) \frac{\cos \theta}{\cos \gamma} \quad (8)$$

By summing the force components in the z-direction, and substituting the expression for F1 in (8), an expression of F2 was obtained as

$$F2 = -F3 + \frac{F4}{\sin \theta} \left(-1 + \frac{\cos \theta \sin \gamma}{\sin \theta \cos \gamma} \right)^{-1} \quad (9)$$

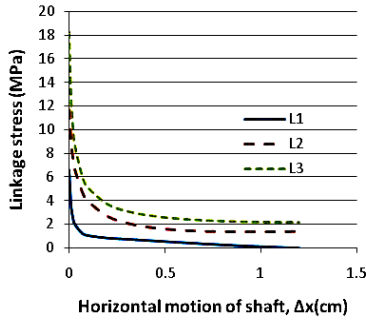


Fig. 10 Plot of theoretical linkage stresses versus forward horizontal motion of the shaft, for a force of 0.508N applied to the tip of a grasper built to scale.

Hence, F3, F2 and F1 were consecutively solved for each jaw opening width for a grasper built to scale. The results predicted for linkage stresses are shown in Fig. 10. The maximum linkage stress of 18.3MPa was found to be on the linkage closest to the grasper jaws when the jaws are fully closed. As the tensile strength of surgical stainless steel is at least an order of magnitude higher than the maximum stress, risk of linkage fracture was considered reasonably small.

Analysis of pin joint stresses Several types of pin joint stresses exist for the pin joints designed in our prototype: (i) Shear stress on the pin, (ii) tensile stress on the member, (iii) compressive stress on the member and (iv) tear out failure. The predicted pin joint stresses were calculated assuming a force at the tip of the grasper jaw of 0.508N as before. In all cases, the pin joint stress was evaluated to be less than 30MPa. Since the tensile strength of surgical stainless steel is at least an order of magnitude higher than 30MPa, the risk of joint failure was considered reasonably small.

Analysis of non-parallel play of grasper jaws The parallel motion of the grasper jaws with respect to each other is important for 2 reasons. Firstly, it allows for equal force

distribution across the grasper jaws. Secondly, if the grasper jaws are not parallel to each other when fully closed, it results in a tiny gap at the tip of the grasper jaws, which can impede the user's efforts to grip a thin piece of tissue with the tip of the grasper. Unfortunately, as allowance between the linkage head and pin is inbuilt into pin joints to provide room for pivoting, some non-parallel motion of the jaws is always possible. The maximum deviation of the grasper jaws from the horizontal depends only on the lengths of 4 of the linkages – L2, 3, 5 and 6 – and the diameters of the holes and pins related with each link. As an example, the method used to calculate the shortest possible length of L2, L2*, is shown in Fig. 11, using the equation as follows:

$$L2^* = L2 - \Delta L2 - 2\left(\frac{\Delta d21}{2} + \frac{\Delta d22}{2}\right) \quad (10)$$

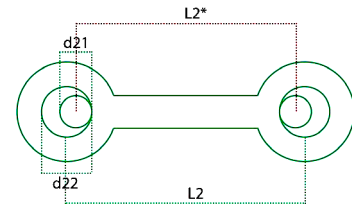


Fig. 11 Illustration of method used to calculate shortest possible length of L2, L2*.

Conversely, the longest possible length of L2, L2**, could be calculated as:

$$L2^{**} = L2 + \Delta L2 + 2\left(\frac{\Delta d21}{2} + \frac{\Delta d22}{2}\right) \quad (11)$$

The maximum play at the grasper tip for each jaw opening width can thus be calculated using the shortest length for L2 and L6, and the longest length got L3 and L5 (Fig. 12).

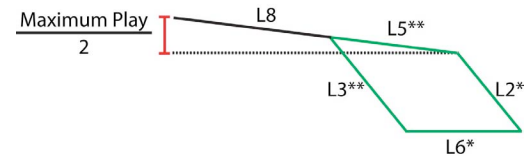


Fig. 12 Illustration of scenario in which maximum play of the grasper tip is achieved (see text for details).

Based on this method, the maximum play at the tip predicted for the 2x prototype was plotted (Fig. 13). Play is greatest when the grasper jaws are fully closed, i.e. there is no horizontal motion of the shaft.

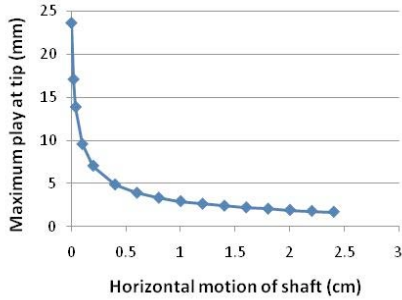


Fig. 13 Plot of maximum play at the grasper tip versus horizontal motion of the shaft for the 2x prototype.

EMPIRICAL VALIDATION OF ANALYSIS

To ensure that the predictions of the laparoscopic grasper were accurate, various tests were performed on the grasper. Before testing, all grasper components were measured to ensure that they met accuracy and tolerance specifications. For our 2x prototypes, all of the lengths, widths and hole tolerances met our specifications.

We first tested the relation between the horizontal movement of the shaft and jaw opening width. The shaft was displaced forward various distances, and the distance between the inner surfaces of the grasper jaw tips was measured for each displacement. The results of these measurements can be seen in Fig. 7. The empirical results were very close to our analytical predictions, confirming that the linkages were functioning as designed and predicted.

Next, we tested the relationship between the horizontal motion of the jaws and the movement of the horizontal shaft. We predicted that the horizontal displacement of the grasper jaws would be 3.93mm when fully opened (Fig. 8). As expected, our tests confirmed that the horizontal motion of the grasper jaws were less than 5mm. Hence, the linkage design was shown to provide almost purely vertical motion of the grasper jaws.

Next, we tested the play experienced at the tip of the jaw. Our empirical results were within our theoretical predictions. Play was measured by forcing the grasper jaw tips open while the ends of the grasper jaw (nearer to the shaft) were held closed. The play measured at the tip of the jaws was 1.0 cm (Table 1). Although 1.0 cm of play is greater than the ideal play (i.e. the play if all grasper components were manufactured exactly according to design), the result fell within the range bracketed by the expected play, and the play in the worst case scenario. Since the result was closer to the expected play, we were satisfied that the play of the tip is predictable, and can be minimized in future improved designs.

Table 1 Theoretical predictions for play experienced at grasper tips as compared to the actual play for the 2x prototype

Play at tip(cm) when fully closed	
Ideal	0.234
Expected	0.589
Worst case scenario	2.364
Actual	1.0

Finally, we tested the relation of the force at the tip to the force at the shaft. To perform this test, it was important to control the force used to close the grasper and the width of jaws opening. To achieve this, weights of 1.25, 2.5, 3.75, and 5 lb were hung from the shaft of the grasper, while spacers of 0.75 cm, 2.75 cm and 5 cm held jaws open at a constant width. A calibrated flexi-force sensor was then placed at the center of the grasper jaws to sense the force exerted there for each weight and jaw opening width. The predicted and empirical results can be seen in Fig. 14.

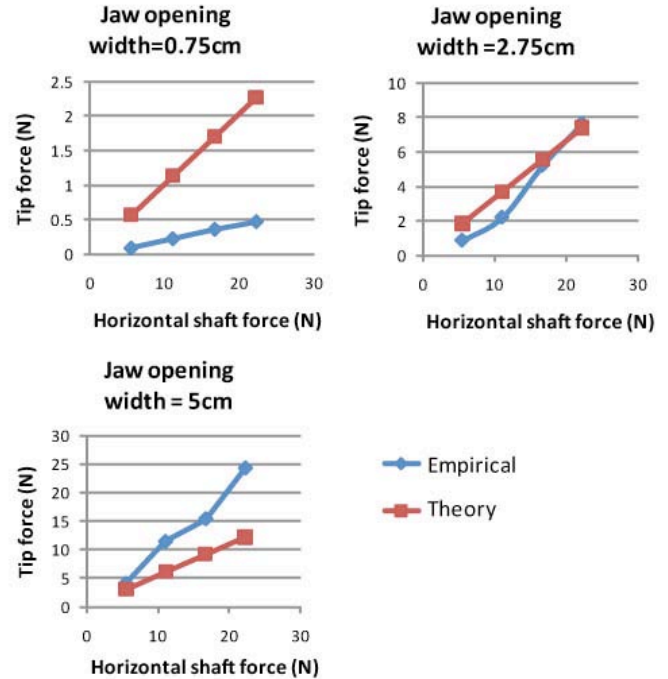


Fig. 14 Plot of force generated at the tip of the grasper jaws versus the force on the shaft, for 3 different jaw opening widths (0.75, 2.75 and 5cm). Empirical data (blue) was compared against theoretical data (red).

The empirical results were relatively accurate for the jaw opening widths of 2.75 and 5 cm. For the width of 0.75 cm, the empirical results had a greater disagreement with theoretical predictions mainly because due to play at the tip. We believe that this play reduced the force exerted at the tip, especially at the 0.75 cm jaw opening width. As previously mentioned, this play is not favorable in a surgical setting where thin pieces of tissue must sometimes be grasped. However, this play can be eliminated with tighter tolerances and the use of flexures instead of linkages.

CONCLUSION AND FUTURE WORK

The knowledge gained from the analysis, fabrication, and testing of the 2x scale prototype has proven to be very promising. Future work will focus on various details.

For grasper design, the possible use of flexures instead of links with pin joints will be explored. Flexures could both

reduce play in the system as well as ease manufacturing and assembly. Furthermore, it is worth investigating the performance of jaws with non-parallel motion. It may be possible to counter the inevitable play in the linkage by shortening the two front-most links, allowing the grasper to apply a closing force in the fully closed position. An elastic guard that keeps tissue from getting pinched in the pin joints and links will also be necessary. This guard should expand and contract as the jaws open and close. The circuitry should also be sized to fit a battery comfortably inside the handle. A professionally printed circuit board should eliminate this problem.

Finally, it is necessary to build a 1x scale version of the entire grasper. Refinements to the handle and trigger design will certainly accompany a smaller scale model in order to make it more comfortable to use as well as to accommodate the smaller jaw closing distance. *Ex vivo* testing on healthy animal bowel tissue will be required to more definitively show that our grasper can reduce tissue trauma during laparoscopic surgery.

In conclusion, we present a strong proof-of-concept of a laparoscopic grasper with incorporates parallel jaw design, force feedback (via vibrotactile and visual cues) and ergonomic handle design. The mechanism has predictable motion and force characteristics, and the parallel jaws facilitate easy gripping of tissue, and force feedback minimizes the risk of tissue trauma. As the circuitry of the device is relatively simple and can be powered by a standard household 9V battery, the grasper can be made cost appropriate and disposable. Future work will focus mainly on reducing play at the grasper tip, and *ex vivo* animal testing with the ultimate aim of clinical translation.

ACKNOWLEDGEMENT

The design and fabrication of this device was a term project in MIT 2.75 Precision Machine Design Course and was supported by the Center for Integration of Medicine and Innovative Technology www.cimit.org under U.S. Army Medical Research Acquisition Activity Cooperative Agreement W81XWH-09-2-0001. The information contained herein does not necessarily reflect the position or policy of the Government, and no official endorsement should be inferred. Special thanks are due to Nevan Hanumara, David Custer and Nikolai Begg for their guidance throughout the project.

REFERENCES

1. Westebring - van der Putten, E.P., et al., *The Effect of Augmented Feedback on Grasp Force in Laparoscopic Grasp Control*. Haptics, IEEE Transactions on, 2010. **3**(4): p. 280-291.
2. MacFarlane, M., et al., *Force-feedback grasper helps restore sense of touch in minimally invasive surgery*. Journal of Gastrointestinal Surgery, 1999. **3**(3): p. 278-285.
3. Akinbiyi, T., et al. *Dynamic Augmented Reality for Sensory Substitution in Robot-Assisted Surgical Systems*. in *Engineering in Medicine and Biology Society, 2006. EMBS '06. 28th Annual International Conference of the IEEE*. 2006.

4. Bethea, B.T., et al., *Application of Haptic Feedback to Robotic Surgery*. Journal of Laparoendoscopic & Advanced Surgical Techniques, 2004. **14**(3): p. 191-195.
5. Westebring-van der Putten, E.P., et al., *Force feedback requirements for efficient laparoscopic grasp control*. Ergonomics, 2009. **52**(9): p. 1055 - 1066.
6. Westebring-van der Putten, E., et al., *The opinion and experience of surgeons with laparoscopic bowel grasper haptics*. Journal of Biomedical Science and Engineering, 2010. **3**(4): p. 422-429.
7. Heijnsdijk, E., et al., *The influence of force feedback and visual feedback in grasping tissue laparoscopically*. Surgical Endoscopy, 2004. **18**(6): p. 980-985.
8. Griffiths, J.R., *Laparoscopic Instrument with Parallel Actuated Jaws*, U.S.P. Office, Editor. 2001: United States.
9. Mirbagheri, A. and F. Farahmand. *Design and analysis of an actuated endoscopic grasper for manipulation of large body organs*. in *Engineering in Medicine and Biology Society (EMBC), 2010 Annual International Conference of the IEEE*. 2010.
10. Frank, T.G. and A. Cuschieri, *Prehensile atraumatic grasper with intuitive ergonomics*. Surgical Endoscopy, 1997. **11**(10): p. 1036-1039.
11. Vonck, D., et al., *Vacuum grasping as a manipulation technique for minimally invasive surgery*. Surgical Endoscopy. **24**(10): p. 2418-2423.
12. Marucci, D.D., et al., *A compliant tip reduces the peak pressure of laparoscopic graspers*. ANZ Journal of Surgery, 2002. **72**(7): p. 476-478.
13. Fries, R.C., *Reliable Design of Medical Devices*. 2nd ed. 2006, Boca Raton: Taylor and Francis.
14. *Tekscan Pressure Sensors*. 2010 [cited 2010 Dec 12]; Available from: <http://tekscan.com/pressure-sensors>.
15. Sanders, M.S. and E.J. McCormick, *Human Factors in Engineering and Design*. 1993, New York: McGraw-Hill.
16. Marcos, P.F., et al., *Anatomic Bladder Neck Preservation During Robotic-Assisted Laparoscopic Radical Prostatectomy: Description of Technique and Outcomes*. European Urology, 2009. **56**(6): p. 972-980.